Surface plasmon polaritons of symmetric and asymmetric metamaterial slabs*

Zhang Hui-Fang(张惠芳)†, Cao Di(曹 迪), Tao Feng(陶 峰), Yang Xi-Hua(杨希华), Wang Yan(王 燕), Yan Xiao-Nan(阎晓娜), and Bai Li-Hua(白丽华)

Department of Physics, Shanghai University, Shanghai 200444, *China*

(Received 14 April 2009; revised manuscript received 1 July 2009)

The p and s-polarized surface plasmon polaritons (SPPs) of symmetric and asymmetric slabs formed arbitrarily by four types of conventional materials: dielectrics, negative dielectric permittivity materials, negative magnetic permeability materials, and left-handed materials are comprehensively analysed. The existence regions, dispersion relations, and excitation of SPPs in different frequency regions are investigated in detail. For symmetric slabs, the numbers and the frequency positions of surface polariton branches are quite different. At the same time, the pairs of the p or s-polarized SPP branches occur in the same frequency range. For asymmetric slabs, the SPP branches in mid- and high-frequency ranges are greatly different. In addition, the slab thickness has a great effect on SPPs of asymmetric and symmetric slabs. The attenuated total reflection spectra for the cases of p and s polarizations in these slabs are also calculated.

Keywords: surface plasmon polaritons, meta-materials, symmetric and asymmetric slabs, attenuated total reflection technique

PACC: 7320M, 4265, 9130F, 4110H

1. Introduction

Russian scientist Victor Veselago predicted very unusual electromagnetic (EM) properties for a hypothetical material with simultaneously negative dielectric permittivity and negative magnetic permeability in a certain frequency range.[1] This material is consequently dubbed left-handed medium (LHM) since the wave vector, the electric field vector, and the magnetic field vector form a left-handed system when a plane EM wave propagates in it. Pendry's group designed skillfully the negative dielectric permittivity material (NDPM) constructed by thin metallic wire network, and the negative magnetic permeability medium (NMPM) composed of a periodic arrangement of split ring resonators (SRRs).[2−4] Later, Smith *et al.* experimentally demonstrated the first LHM by means of combination of the periodic arrangements of nonmagnetic split ring resonators and thin metallic wires.[5,6] LHM has some possible applications in the design of novel photoelectric devices, antennas and waveguides used in wireless communications,[7−10] optical communications,[11−14] and medical diagnostic system.[14]

Surface plasmon polaritons (SPPs) have aroused the interest of scientists including physicists, chemists and materials scientists and biologists. SPP is a kind of surface wave that propagates along the interface and decays in the transverse direction exponentially. SPPs were explored for their potential applications in subwavelength optics, data storage, light generation, microscopy and bio-photonics.[15] Thus the investigations of SPPs propagating along various interfaces are important in the sense of both basic research and practical application,[16−20] especially those that are associated with LHM owing to their numerous possible applications and unexpected properties.[21−26] In addition, the slabs of LHMs could be employed as an unconventional alternative to lenses for focusing both propagating and evanescent waves.[27]

In the present paper, we study the p and the s-polarized SPPs of symmetric and asymmetric slabs formed arbitrarily by four types of different materials: dielectrics, NDPMs, NMPMs, and LHMs. We examine several symmetric and asymmetric slabs. We find that SPPs of different slabs have quite different properties, i.e. the existence regions, the dispersion relation, and the excitation of SPPs depend on the composite materials and the thickness of slab, the parameters of metamaterials, etc. For some possible applications, the SPPs of metamaterials slabs could be

*Project supported by the Science Foundation of Shanghai Education Committee, China (Grant No. 06AZ092).

†Corresponding author. E-mail: hfzhang1967@staff.shu.edu.cn

© 2010 Chinese Physical Society and IOP Publishing Ltd

used for novel lenses filter, etc. However, we must note that all the media considered in this paper are homogeneous and isotropic, i.e. in the effective medium approximation if the wavelength of the EM wave is much larger than the period of the artificial metamaterials

2. Dispersion relations of SPPs of a slab

We consider the slab made of three media 1, 2 and 3. Medium 2 with the permittivity ε_2 and permeability μ_2 occupies the region $0 < x < d$. Medium 1 with the permittivity ε_1 and permeability μ_1 occupies the $x < 0$ semi-infinite space and the region of $x > d$ is occupied by medium 3 with the permittivity ε_3 and permeability μ_3. Note that a lossless case is considered in the following and $\varepsilon_{1,2,3}$ and $\mu_{1,2,3}$ are allowed to be positive or negative.

We derive the dispersion relations of SPPs for a slab. To start with, we discuss the p polarization case. In the region $x < 0$, the electromagnetic fields have the form:

$$\boldsymbol{H}_1 = A\hat{y}\,\mathrm{e}^{k_1 x}\mathrm{e}^{\mathrm{i}\,hz}, \tag{1}$$

$$\boldsymbol{E}_1 = \frac{c}{\omega\varepsilon_1}A(h\hat{x} + \mathrm{i}\,k_1\hat{z})\,\mathrm{e}^{k_1 x}\mathrm{e}^{\mathrm{i}\,hz}. \tag{2}$$

For the fields in the region $0 < x < d$, we use the form

$$\boldsymbol{H}_2 = \hat{y}(B\,\mathrm{e}^{-k_2 x} + C\,\mathrm{e}^{k_2 x})\,\mathrm{e}^{\mathrm{i}\,hz}, \tag{3}$$

$$\boldsymbol{E}_2 = \frac{c}{\omega\varepsilon_2}[B(h\widehat{x} - \mathrm{i}\,k_2\widehat{z})\,\mathrm{e}^{-k_2 x} + C(h\hat{x} + \mathrm{i}\,k_2\hat{z})\,\mathrm{e}^{k_2 x}]\,\mathrm{e}^{\mathrm{i}\,hz}. \tag{4}$$

In the region $x > d$ the fields are written in the form

$$\boldsymbol{H}_3 = D\hat{y}\,\mathrm{e}^{k_3 x}\,\mathrm{e}^{\mathrm{i}\,hz}, \tag{5}$$

$$\boldsymbol{E}_3 = \frac{c}{\omega\varepsilon_3}D(h\hat{x} - \mathrm{i}\,k_3\hat{z})\,\mathrm{e}^{k_3 x}\,\mathrm{e}^{\mathrm{i}\,hz}. \tag{6}$$

Here $\hat{x}$, $\hat{y}$ and $\hat{z}$ are unit vectors in the x, y and z directions, respectively. $k_{1,2,3}$ are the attenuation coefficients of the surface polariton fields in the normal direction x of the interface, which can be written as

$$k_{1,2,3}^2 = h^2 - \varepsilon_{1,2,3}\mu_{1,2,3}\omega^2/c^2, \tag{7}$$

where h is the wave-vector component along propagation direction z. The nature of surface waves requires $k_{1,2,3}$ to be real and positive, so

$$h^2 > \max[\varepsilon_1\mu_1(\omega/c)^2, \varepsilon_2\mu_2(\omega/c)^2, \varepsilon_3\mu_3(\omega/c)^2]. \tag{8}$$

By using the electromagnetic boundary conditions at the interfaces $x = 0$ and $x = d$ the dispersion relation of the p-polarized SPP is derived as[28]

$$\frac{(k_2/\varepsilon_2 - k_1/\varepsilon_1)(k_2/\varepsilon_2 - k_3/\varepsilon_3)}{(k_2/\varepsilon_2 + k_1/\varepsilon_1)(k_2/\varepsilon_2 + k_3/\varepsilon_3)} = \mathrm{e}^{2k_2 d}. \tag{9}$$

In the same way, the dispersion relation of the s-polarized SPPs can be obtained to be

$$\frac{(k_2/\mu_2 - k_1/\mu_1)(k_2/\mu_2 - k_3/\mu_3)}{(k_2/\mu_2 + k_1/\mu_1)(k_2/\mu_2 + k_3/\mu_3)} = \mathrm{e}^{2k_2 d}. \tag{10}$$

From expressions (9) and (10) it follows that the dispersion relations of SPPs are the same if we exchange medium 1 and medium 3 (i.e. exchange ε_1, μ_1 and ε_3, μ_3), and keep the physical property of medium 2 unchanged. If the slab is symmetric (i.e. $\varepsilon_1 = \varepsilon_3$, $\mu_1 = \mu_3$), expressions (9) and (10) can be simplified into expressions (11), (12), (19) and (20) in Ref. [22].

We have discussed the dispersion relations and the existence conditions of SPPs for p and s polarizations at the interface formed by arbitrary two media and found that SPPs originated from the uncontinuous jump of permittivity from positive value to negative one at the interface for the p polarization and the discontinuous jump of permeability from positive value to negative one at the interface for the s polarization.[29]

In the following, by numerical calculation, we discuss the SPPs of several symmetric and asymmetric slabs respectively.

3. SPPs of symmetric slab

Here, we assume that media 1–3 are any ones of the four different materials, which are LHMs, NDPMs, NMPMs, and dielectrics. The relations between the physical properties of these four types of materials and frequency were discussed in Ref. [30]. In Eqs. (13)–(16) of Ref. [30], the various parameters are set as follows: $\omega_p = 10.0$ GHz, $\omega_0 = 4.0$ GHz, $F_1 = 0.56$, $F_2 = 1.25$, $\omega_a = 6.0$ GHz, and $h_0 d = 0.5$, where $h_0 = \omega_0/c$ (all angular frequencies are scaled by 2π in this paper), which are in agreement with those of the experimental implementation.[5] For convenience, we use Re[ ] to describe the real parts of physical parameters , i.e. we neglect their damping terms when we discuss the existence regions and dispersion relation of SPPs.

3.1. SPPs of the LHM-dielectric-LHM symmetric slab

We assume that medium 2 is a dielectric, and media 1 and 3 are the LHM.

3.1.1. Existence region and dispersion relation of SPPs

We investigate the existence regions and dispersion-relation curves of SPPs in plane (h, ω) as shown in Fig. 1. The dash curve (i) and the dash line (ii) correspond to $h = (\varepsilon_1\mu_1)^{1/2}(\omega/c)$ and $h = (\varepsilon_2\mu_2)^{1/2}(\omega/c)$, respectively, where ε_1 and μ_1 are determined by expressions (13) and (14) in Ref. [30], and ε_2 and μ_2 are 1. The dot lines (iii) and (iv) correspond to $\omega = \omega_0$ and $\omega = (1-F_1)^{-1/2}\omega_0$, respectively.

According to the existence conditions of SPPs,[29] there are three regions of R1, R2 and R3, in which SPPs can exist (Fig. 1). R1 is on the right-hand side of line (ii) and below line (iii) when $\omega < 4.0$ GHz; R2 is the region encircled by line (ii), curve (i) and line (iv) when 4.0 GHz $< \omega <$ 6.0 GHz; and R3 is on the right-hand side of line (ii) and above line (iv) when 6.0 GHz $< \omega <$ 10.0 GHz. These three regions of R1, R2 and R3 correspond to the three kinds of interface structures as metal–dielectric–metal, LHM–dielectric–LHM, and metal–dielectric–metal, respectively. As to the types of SPPs these regions support, we can see that the regions R1 and R3 in Fig. 1 support only two p-polarized SPPs, because only the permittivity changes from negative value to positive one across the metal–dielectric interface. The region R2 in Fig. 1 supports both polarized SPPs because the permittivity and the permeability both change their signs across the LHM–dielectric interface. Thus, in region R2, the unusual property of possessing surface localized modes exists within the frequency pass band (in which both the permittivity and the permeability are simultaneously negative or positive).

Next, we discuss the dispersion relation curves of SPPs, obtained by solving expressions (9) and (10), and the results are also shown in Fig. 1. We obtain four dispersion curves (P1), (P2), (P3), and (P4) for p-polarized SPPs, and two dispersion curves, (S1) and (S2), for s-polarized SPPs as shown in Fig. 1. Branches (P1) and (P2) are in region R1 in a low frequency range. Part of branch (P3) is in a region of R2, and the rest is in a region of R3. The branch (P4) occurs in a region R3. Branches (S1) and (S2) lie completely inside the region of R2.

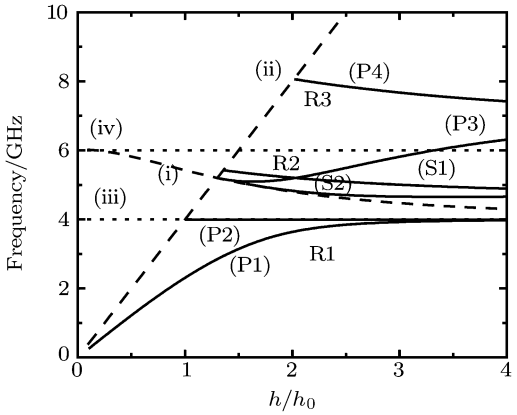


Fig. 1. Existence regions and dispersion relation curves of SPPs in plane (h/h_0, ω) for the LHM–dielectric–LHM symmetric slab with thickness $h_0 d = 0.5$. Curve (i) is $h = (\varepsilon_1\mu_1)^{1/2}(\omega/c)$, line (ii) is $h = (\varepsilon_2\mu_2)^{1/2}(\omega/c)$, line (iii) is $\omega = \omega_0$, and line (iv) is $\omega = (1-F_1)^{-1/2}\omega_0$. h is in units of $h_0 = \omega_0/c$. R1, R2 and R3 denote the three regions in which SPPs can exist. The surface polariton branches (P1), (P2), (P3), and (P4) are for p polarization and branches (S1) and (S2) are for s polarization.

3.1.2. ATR spectra for SPPs

SPP is a kind of surface wave that propagates along an interface with amplitudes decaying exponentially away from the interface. Its wavevector is always larger than those of the bulk EM waves in the two media across the interface. Due to this wave-vector mismatch, SPPs will not interact directly with an incoming EM plane wave. However, they can be excited in a layered structure containing a prism with high refractive index, i.e. attenuated total

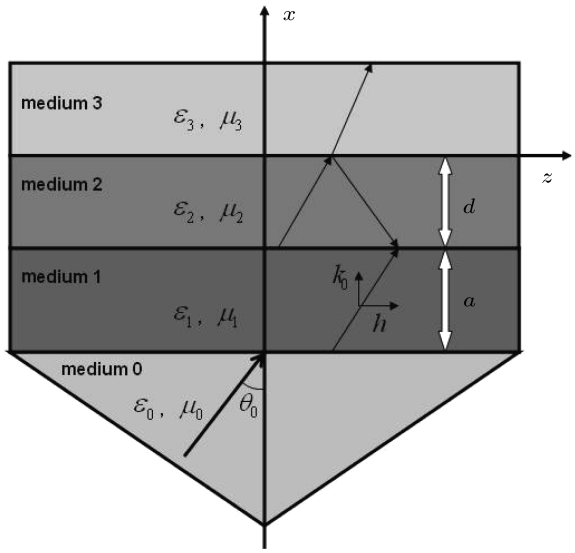


Fig. 2. Configuration of a dielectric prism for the ATR spectra study.

reflection (ATR), through the evanescent field tunneling effect. For this method, two schemes are frequently used: the Otto configuration[16] and the Kretschmann configuration.[31] The ATR geometry under consideration is shown in Fig. 2, in which a dielectric prism labeled as the medium 0 is placed under medium 1 and has frequency-independent permittivity ε and permeability μ. Thus, these four media comprise a four-layered structure, in which media 3 and 0 can be considered to be semi-infinite, medium 1 has a finite thickness of a, and medium 2 has a finite thickness of d.

By using the classical electromagnetic theory, we have calculated the complex amplitude reflectivity of the arbitrary slab.[28] In all calculations, four damping parameters in expressions (13)–(16) in Ref. [30] were always chosen to be $\gamma = 0.03\omega_p$, $\Gamma_1 = 0.03\omega_0$, $\gamma_a = 0.03\omega_a$, and $\Gamma_2 = 0.02\omega_0$. For the case of p polarization, with the thickness of medium 1, a, being 0.1 cm, i.e. $a = 0.1$ cm, and thickness of medium 2, $h_0 d$, being 0.5, i.e. $h_0 d = 0.5$, the calculated ATR spectra are shown in Fig. 3(a) at incident angle $\theta = 60°$. In Fig. 3(a), we can observe that four sharp absorption peaks denoted by S_p are due to SPPs. The two low-frequency peaks at ∼0.36 GHz and ∼3.84 GHz, correspond to the branches P1 and P2 in Fig. 1, respectively, and the two high-frequency peaks at ∼6.58 GHz and ∼8.41 GHz are due to the high frequency branches P3 and P4 in Fig. 1. For the case of s polarization, at incident angle $\theta = 60°$, the ATR spectra in the same frequency regimes with $a = 0.1$ cm are plotted in Fig. 3(b). We find that one bulk mode absorption denoted by B at ∼4.07 GHz, two surface mode peaks denoted by S_s at ∼4.76 GHz and ∼5.48 GHz, correspond to the branches (S1) and (S2) in Fig. 1 respectively. The peak denoted by B lies outside the frequency range of the surface polariton branches, and it is due to the excitation of a non-radiative bulk polariton, i.e. a polariton that has a sinusoidal behaviour in the x direction inside the slab, and an exponential decay outside the slab.[32]

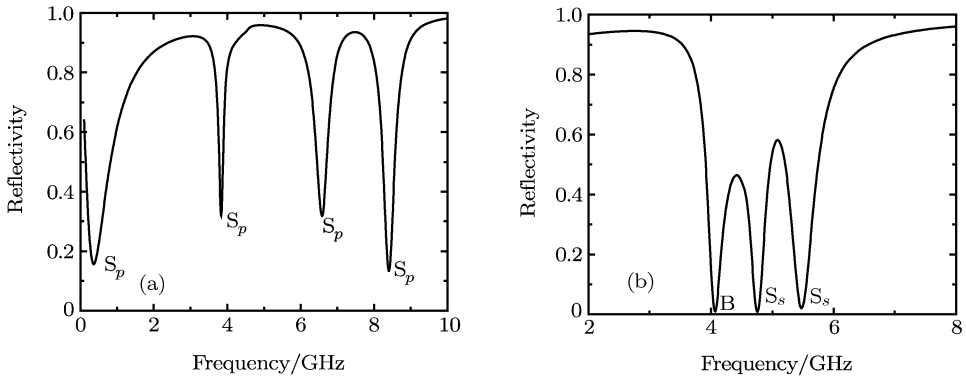


Fig. 3. ATR spectra for exciting and observing SPPs in the frequency regime for the LHM–dielectric–LHM symmetric slab. Panel (a) is for the p-polarization case, and panel (b) for the s-polarization case. The parameters used in these calculations are $\varepsilon_0 = 8.0$, $\mu_0 = 1.0$, $a = 0.1$ cm, $h_0 d = 0.5$, $\theta_0 = 60°$.

In contrast with the dielectric–LHM–dielectric slab,[22] the frequency positions of surface polariton branches of the LHM–dielectric–LHM slab shift a little. It has been suggested that the dielectric–LHM–dielectric slab could be employed as convex lenses.[27] So the LHM–dielectric–LHM slab maybe serves as a concave lens.

3.2. SPPs of NDPM–LHM–NDPM symmetric slab

In this case we assume that medium 2 is an LHM, and media 1 and 3 are the NDPM.

3.2.1. Existence region and dispersion relation of SPPs

Figure 4 shows the existence regions and dispersion-relation curves of SPPs in plane (h, ω). The dash curves (i) and (ii) correspond to $h = (\varepsilon_1\mu_1)^{1/2}(\omega/c)$ and $h = (\varepsilon_2\mu_2)^{1/2}(\omega/c)$, respectively, where ε_1, ε_2 and μ_2 are determined by expressions (15), (13), and (14),[30] in Ref. [30] and μ_1 is 1. The dot lines (iii), (iv) and (v) correspond to $\omega = \omega_0$, $\omega = (1 - F_1)^{-1/2}\omega_0$ and $\omega = \omega_p = 10.0$, respectively.

In Fig. 4, there are two regions, i.e., R1 and R2 in which the excitation of SPPs is possible according to inequality (8). Region R1 is above curve (ii) and below line (iv) when 4.0 GHz$< \omega <$ 6.0 GHz, and it is the interfaces of metal–LHM–metal owing to the fact that Re$[\varepsilon_1(\omega)] < 0$, $\mu_1 > 0$ and Re$[\varepsilon_2(\omega)] < 0$, Re$[\mu_2(\omega)] < 0$. Two s-polarized SPPs (i.e. curves (S1) and (S2) in Fig. 4) can be excited because only the magnetic permeability changes its sign across the metal–LHM–metal interfaces in region R1. Region R2 is bounded by the right-hand side of curve (i) and upside of line (iv) when 6.0 GHz$< \omega <$ 10.0 GHz, and it is the interfaces of dielectric–metal–dielectric since Re$[\varepsilon_2(\omega)] < 0$, Re$[\mu_2(\omega)] > 0$, Re$[\varepsilon_1(\omega)] > 0$ and $\mu_1 > 0$. According to the existence conditions of SPPs,[29] two p-polarized SPPs (i.e. curves (P1) and (P2) in Fig. 4) are supported in this region. It should be pointed out that the surface polariton branches only occur in the region 4.0 GHz$< \omega <$ 10.0 GHz. In the regions $\omega <$ 4.0 GHz and $\omega >$ 10.0 GHz, no SPPs can be found since the permittivity and the permeability do not change their signs across the dielectric–dielectric–dielectric interfaces. So, in the above two regions, surface polaritons exist only in the frequency stop band.

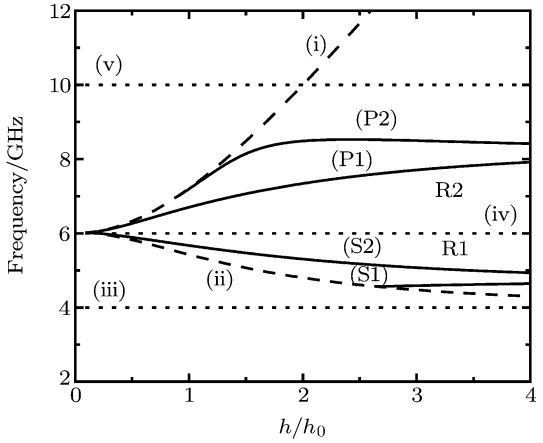


Fig. 4. The same as Fig. 1. The symmetric slab is comprised of NDPM, LHM, and NDPM. Curve (i) is $h = (\varepsilon_1\mu_1)^{1/2}(\omega/c)$, curve (ii) is $h = (\varepsilon_2\mu_2)^{1/2}(\omega/c)$, and line (v) is $\omega = \omega_p$. R1 and R2 denote the two existence regions of SPPs. The branches (P1) and (P2) are for p polarization and branches (S1) and (S2) are for s polarization.

3.2.2. ATR spectra for SPPs

With numerical calculations, we depict the ATR spectra for the cases of p and s polarizations in the frequency regime in Fig. 5(a) and 5(b), respectively. For the case of p-polarization, at incident angle $\theta_0 = 60°$ and with $a = 0.1$ cm and $h_0 d = 0.5$, the ATR spectra are shown in Fig. 5(a). There appear three sharp absorption peaks, two of them, denoted by S_p at $\sim$ 7.13 GHz and $\sim$ 8.25 GHz, correspond to the p-polarized branches P1 and P2 in Fig. 4, the last of them, denoted by B at $\sim$ 4.20 GHz, is bulk absorption peak. For the case of s- polarization, at incident angle $\theta_0 = 60°$ and with $a = 0.2$ cm and $h_0 d = 0.5$, the ATR spectra are shown in Fig. 5(b). In Fig. 5(b), we find two absorption peaks denoted by S_s at $\sim$ 4.43 GHz and $\sim$ 5.02 GHz to correspond to branches S1 and S2 in Fig. 4, respectively, and one bulk mode absorption denoted by B at $\sim$ 4.08 GHz.

From the above discussion, for these two typical symmetric slabs, we find that the numbers and frequency positions of surface polariton branches are quite different. At the same time, we also observe that the pairs of the p- or s-polarized SPP branches occur in the same frequency range because the jumps of the permittivity and the permeability from positive to negative are the same across the two surfaces of the symmetric slabs.

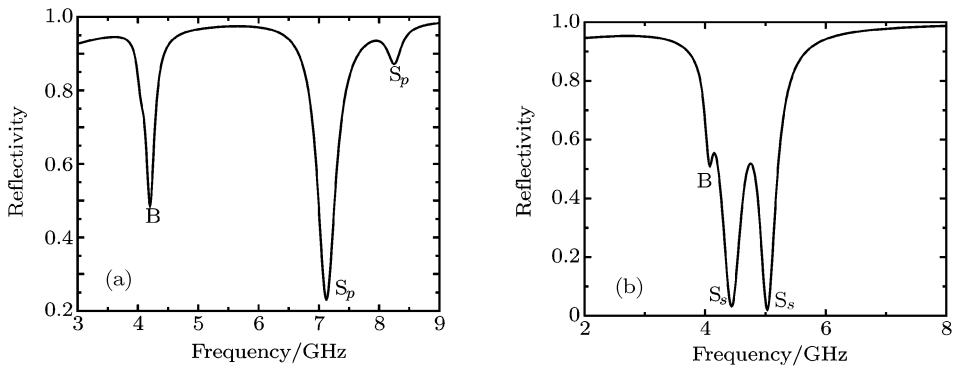


Fig. 5. The same as Fig. 3. The symmetric slab is comprised of NDPM, LHM, and NDPM. Panel (a) shows the p polarization with $a = 0.1$ cm and panel (b) displays the s polarization with $a = 0.2$ cm.

4. SPPs of asymmetric slab

4.1. SPPs of the LHM–dielectric–NMPM asymmetric slab

We assume that media 1, 2 and 3 are LHM, dielectric and NMPM, respectively.

4.1.1. Existence region and dispersion relation of SPPs

Figure 6 shows the existence regions and dispersion-relation curves of SPPs in plane (h, ω). The dash curve (i), line (ii) and curve (iii) correspond to $h = (\varepsilon_1\mu_1)^{1/2}(\omega/c)$, $h = (\varepsilon_2\mu_2)^{1/2}(\omega/c)$ and $h = (\varepsilon_3\mu_3)^{1/2}(\omega/c)$, respectively, where ε_1, μ_1, and μ_3 are determined by expressions (13), (14), and (16),[30] and ε_2, μ_2 and ε_3 are 1. The dot lines (iv) and (v) correspond to $\omega = \omega_0$ and $\omega = (1-F_1)^{-1/2}\omega_0$, respectively.

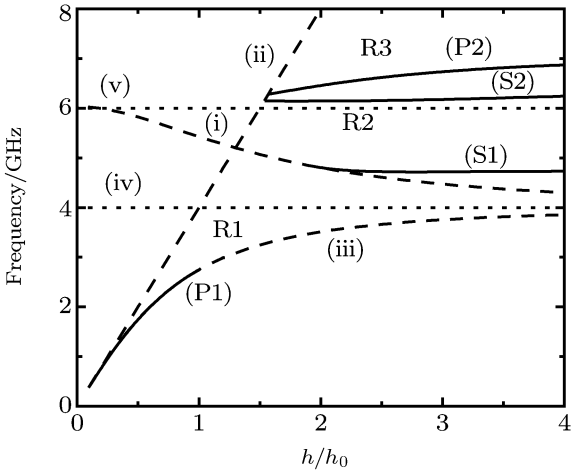


Fig. 6. The same as Fig. 1. The asymmetric slab is comprised of LHM, dielectric, and NMPM. Curve (i) is $h = (\varepsilon_1\mu_1)^{1/2}(\omega/c)$, line (ii) is $h = (\varepsilon_2\mu_2)^{1/2}(\omega/c)$, curve (iii) is $h = (\varepsilon_3\mu_3)^{1/2}(\omega/c)$, line (iv) is $\omega = \omega_0$, and line (v) is $\omega = (1 - F_1)^{-1/2}\omega_0$. R1, R2 and R3 denote the three existence regions of SPPs. The surface polariton branches (P1) and (P2) are for p polarization and branches (S1) and (S2) are for s polarization.

In Fig. 6, inequality (8) determines three regions R1, R2 and R3 in which the excitation of SPPs is possible, where R1 is the region encircled by the upside of curve (iii), the underside of the line (iv), and the right-hand side of the line (ii) when $\omega < 4.0$ GHz; R2 is the region bounded by the right-hand side of the line (ii), the upside of the curve (i) and the underside of the line (v) when 4.0 GHz $< \omega <$ 6.0 GHz; R3 is the region formed by the right-hand side of the line (ii), the upside of the line (v) when 6.0 GHz $< \omega <$ 10.0 GHz. These three regions R1, R2 and R3 in Fig. 6 correspond to the three kinds of interfaces, i.e. metal–dielectric–dielectric, LHM–dielectric–NMPM, and metal–dielectric–NMPM, respectively. R1 supports only one p-polarized SPP, R2 and R3 both support polarized SPPs. The dispersion curves of SPPs obtained from the numerical calculations of dispersion relations (9) and (10) are also shown in Fig. 6. There exist two p-polarized branches of dispersion curves: one is branch (P1) in region R1, the other is branch (P2) in the frequency region 6.0 GHz $< \omega <$ 10.0 GHz. Branches (S1) and (S2) are s-polarized and occur in regions R2 and R3, respectively.

4.1.2. ATR spectra for SPPs

The calculated ATR spectra for the cases of p and s polarizations in the frequency regime are shown in Figs. 7(a) and 7(b), respectively. For the case of p polarization, which is shown in Fig. 7(a), at incident angle $\theta_0 = 45°$ and with $a = 0.4$ cm and $h_0 d = 0.5$, there appear two sharp absorption peaks denoted by S_p at $\sim$ 3.40 GHz and $\sim$ 7.10 GHz, due to branches (P1) and (P2) in Fig. 6, respectively. One bulk mode absorption peak denoted by B is also seen at $\sim$ 4.11 GHz. In the s polarization case as shown in Fig. 7(b), at incident angle $\theta_0 = 60°$ and with $a = 0.5$ cm and $h_0 d = 0.5$, in addition to the bulk mode absorption denoted by B at $\sim$ 4.13 GHz, two surface mode peaks denoted by S_s at $\sim$ 4.80 GHz and $\sim$ 6.30 GHz are observed. These are due to surface polariton branches (S1) and (S2) in Fig. 6, respectively.

Here, it should be noted that the SPPs of the LHM–NMPM–dielectric slab (we have calculated them but not shown their results graphically here) are similar to those of the LHM–dielectric–NMPM slab. There are also two p-polarized SPPs and two s-polarized SPPs, only the frequency positions of surface polariton branches shift a lot. The SPPs of the dielectric–LHM–NMPM slab,[28] especially, the numbers and the frequency positions of surface polariton branches, are quite different from those of the above two slabs. Furthermore, the main difference in SPP occurs in mid- and high-frequency ranges.

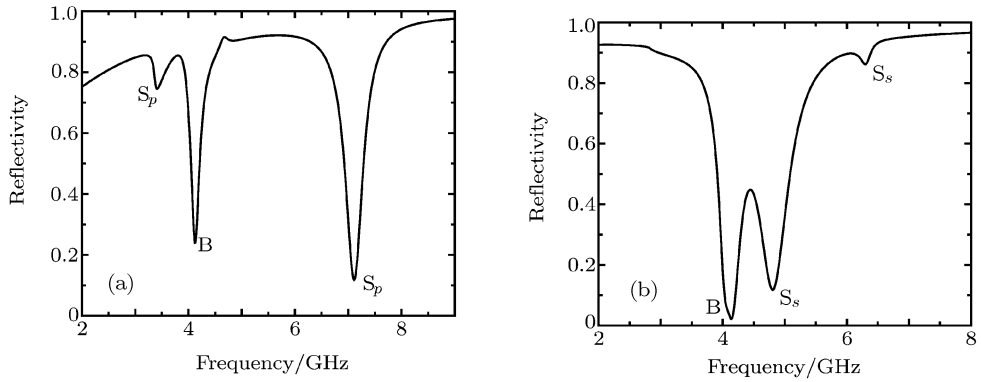


Fig. 7. The same as Fig. 3. The asymmetric slab is comprised of LHM, dielectric, and NMPM. Panel (a) shows the reflectivity for p polarization with $a = 0.4$ cm, $\theta_0 = 45°$, $\varepsilon_0 = 8.0$, and $\mu_0 = 1.0$, and panel (b) displays the reflectivity for s polarization with $a = 0.5$ cm, $\theta_0 = 60°$, $\varepsilon_0 = 3.0$, and $\mu_0 = 1.0$.

4.2. SPPs of LHM–dielectric–NDPM asymmetric slab

We assume that media 1, 2 and 3 are LHM, dielectric and NDPM, respectively.

4.2.1. Existence region and dispersion relation of SPPs

We study the existence regions and dispersion-relation curves of SPPs in plane (h, ω), which are shown in Fig. 8. The dash curve (i), line (ii) and curve (iii) correspond to $h = (\varepsilon_1\mu_1)^{1/2}(\omega/c)$, $h = (\varepsilon_2\mu_2)^{1/2}(\omega/c)$ and $h = (\varepsilon_3\mu_3)^{1/2}(\omega/c)$, respectively, where ε_1, μ_1, and ε_3 are determined by expressions (13)–(15) in Ref. [30] and ε_2, μ_2 and μ_3 are 1. The dot lines (iv) and (v) correspond to $\omega = \omega_0$ and $\omega = (1 - F_1)^{-1/2}\omega_0$, respectively.

In Fig. 8, according to the existence condition of SPPs, there are three regions R1, R2 and R3 in which the SPPs can exist. When $\omega < 4.0$ GHz, the region R1 is comprised by the right-hand side of line (ii) and the underside of line (iv), and it corresponds to the interfaces of metal–dielectric–metal. When 4.0 GHz $< \omega <$ 6.0 GHz, the region R2 is encircled by the right-hand side of line (ii), the upside of curve (i) and the underside of line (v), and it corresponds to the interfaces of LHM–dielectric–metal. When 6.0 GHz $< \omega <$ 10.0 GHz, the region R3 is bounded by the right-hand side of line (ii) and the upside of line (v), and it corresponds to the interfaces of metal–dielectric–dielectric. The dispersion-relation curves of SPPs obtained from the numerical calculations of dispersion relations (9) and (10) are shown in Fig. 8. There exist two p polarized branches of dispersion curves: one is branch (P1) in region R1, and the other is branch (P2) in the frequency region 6.0 GHz $< \omega <$ 10.0 GHz. Branch (S1) is s-polarized and occurs in region R2. Here, it should be pointed out that we can find two p-polarized branches in the low frequency region R1 if we choose the electric plasma frequency ω_a to be 5.0 GHz, i.e. $\omega_a = 5.0$ GHz. We can also see one p-polarized branch in the region R2 if we extend the range of h (i.e. wave vector component along the propagation direction (the z direction) (we have checked them but not shown their results graphically here).

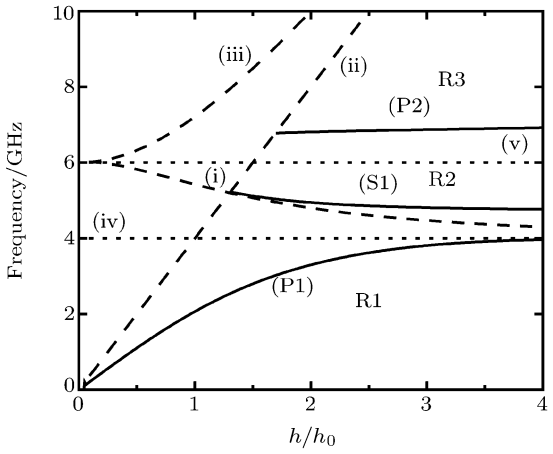


Fig. 8. The same as Fig. 1. Asymmetric slab is comprised of LHM, dielectric, and NDPM. Curve (i) is $h = (\varepsilon_1\mu_1)^{1/2}(\omega/c)$, line (ii) is $h = (\varepsilon_2\mu_2)^{1/2}(\omega/c)$, curve (iii) is $h = (\varepsilon_3\mu_3)^{1/2}(\omega/c)$. R1, R2 and R3 are the three existence regions of SPPs. The surface polariton branches (P1) and (P2) are for p polarization and branch (S1) is for s polarization.

4.2.2. ATR spectra for SPPs

The calculated ATR spectra are shown in Fig. 9. For the case of p polarization as shown in Fig. 9(a), at incident angle $\theta = 60^\circ$ and with $a = 0.6$ cm and $h_0 d = 0.5$, we observe two sharp absorption peaks denoted by S_p at ~ 3.00 GHz and ~ 7.00 GHz, due to branches (P1) and (P2) in Fig. 8, and one bulk mode absorption denoted by B at ~ 4.29 GHz. In the s polarization case as shown in Fig. 9(b), at incident angle $\theta = 45^\circ$ and with $a = 1.0$ cm and $h_0 d = 0.5$, in addition to the bulk mode absorption denoted by B at ~ 4.22 GHz, we find only one surface mode peak denoted by S_s at ~ 4.87 GHz, which is due to surface polariton branch (S1) in Fig. 8.

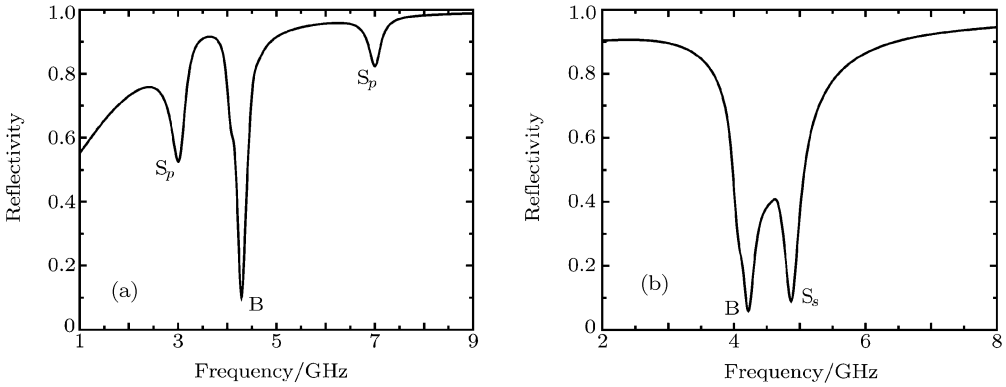


Fig. 9. The same as Fig. 3. Asymmetric slab is comprised of LHM, dielectric and NDPM. Panel (a) shows the reflectivity for p polarization with $a = 0.6$ cm and $\theta_0 = 60^\circ$ and panel (b) displays the reflectivity for s polarization with $a = 1.0$ cm and $\theta_0 = 45^\circ$. The other parameters used are $\varepsilon_0 = 8.0$, and $\mu_0 = 1.0$.

Next, we discuss briefly the SPPs of the LHM–NDPM–dielectric slab (we have calculated them but not shown their results graphically here) there also exist two branches for p-polarized SPPs and one branch for s-polarized SPPs, only the frequency positions of dispersion relation curves shift a little as compared with those of the LHM–dielectric–NDPM slab. As for the SPPs of the dielectric–LHM–NDPM slab,[28] three branches for p-polarized SPPs and two for s-polarized SPPs can be obtained.

4.3. SPPs of NMPM–LHM–NDPM asymmetric slab

We assume that media 1, 2 and 3 are NMPM, LHM and NDPM, respectively.

4.3.1. Existence region and dispersion relation of SPPs

The existence regions and dispersion-relation curves of SPPs in plane (h ω), are shown in Fig. 10. The dash curves (i), (ii) and (iii) correspond to $h = (\varepsilon_1\mu_1)^{1/2}(\omega/c)$, $h = (\varepsilon_2\mu_2)^{1/2}(\omega/c)$, and $h = (\varepsilon_3\mu_3)^{1/2}(\omega/c)$, respectively, where μ_1, ε_2 μ_2 and ε_3 are determined by expressions (16), (13), (14) and (15) in Ref. [30] and ε_1 and μ_3 are 1. The dot lines (iv), (v) and (vi) correspond to $\omega = \omega_0$, $\omega = (1 - F_1)^{-1/2}\omega_0$, and $\omega = \omega_p = 10.0$ GHz, respectively.

In Fig. 10, inequality (8) determines four regions in which the SPPs can exist. Region R1 is bounded by the upside of curve (i) and the underside of line (iv) when $\omega < 4.0$ GHz. Region R2 is encircled by the upside of curve (ii) and the underside of line (v) when 4.0 GHz$< \omega <$ 6.0 GHz. Region R3 is bounded by the right-hand side of curve (iii), the upside of line (v), and the underside of line (vi) when 6.0 GHz$< \omega <$ 10.0 GHz. Region R4 is bounded by the right-hand side of curve (iii) and the upside of line (vi) when $\omega >$ 10.0 GHz. These four regions, R1, R2, R3 and R4, correspond to four kinds of interfaces, i.e. dielectric–metal–metal, NMPM–LHM–metal, NMPM–metal–dielectric, and NMPM–dielectric–dielectric. The dispersion-relation curves of SPPs are also shown in Fig. 10. There exist the following branches: branch (P1), which is p-polarized and occurs in the low frequency region R1; branch (S1), which is s-polarized and occurs in the region R2 in which the slab material is left-handed (in this re-

gion $\mu_2(\omega)$ and $\varepsilon_2(\omega)$ are negative); branches (P2) and (P3), which are p-polarized and occur in the high frequency region R3; branch (S2), which is s-polarized and travels across the high frequency regions R3 and R4.

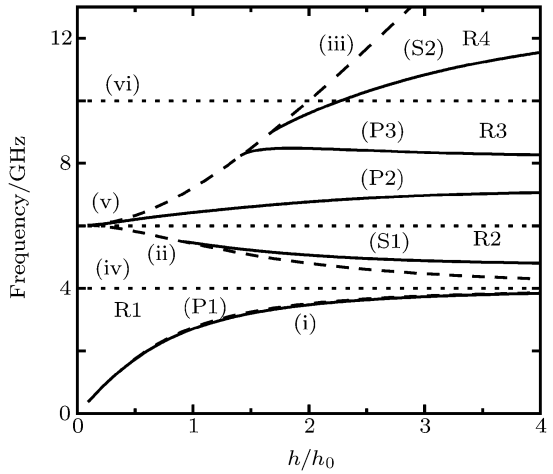


Fig. 10. The same as Fig. 1. Asymmetric slab is comprised of NMPM, LHM, and NDPM. Curve (i) is $h = (\varepsilon_1\mu_1)^{1/2}(\omega/c)$, curve (ii) is $h = (\varepsilon_2\mu_2)^{1/2}(\omega/c)$, curve (iii) is $h = (\varepsilon_3\mu_3)^{1/2}(\omega/c)$ and line (vi) is $\omega = \omega_p$. R1, R2, R3 and R4 are the four existence regions of SPPs. The surface polariton branches (P1), (P2) and (P3) are for p polarization and branches (S1) and (S2) are for s polarization.

4.3.2. ATR spectra for SPPs

With numerical calculations, we depict the ATR spectra in the frequency regime as shown in Fig. 11. For the case of p polarization as shown in Fig. 11(a), at incidental angle $\theta = 45°$ and with $a = 0.5$ cm and $h_0 d = 0.5$, there appear three sharp absorption peaks denoted by S_p at ~ 2.01 GHz, ~ 6.52 GHz, and ~ 8.35 GHz, due to branches (P1), (P2) and (P3) in Fig. 10 respectively. The peak denoted by B at ~ 4.14 GHz is due to bulk mode absorption. For the case of s polarization as shown in Fig. 11(b), at incidental angle $\theta = 45°$ and with $a = 0.4$ cm and $h_0 d = 0.5$, in addition to one bulk mode absorption denoted by B at ~ 4.09 GHz, two absorption peaks denoted by S_s at ~ 5.14 GHz and ~ 10.95 GHz are observed. These are due to branches (S1) and (S2) in Fig. 10 respectively.

In addition, we considered shortly the SPPs of other two slabs comprised of LHM, NDPM and NMPM in a sequence different from the above (we have calculated them but not shown their results graphically here). About the SPPs of these three slabs, it is found that they all have three branches for p-polarized SPPs and two for s-polarized SPPs, but the frequency positions of dispersion relation branches shift a lot, especially, the branches in mid- and high-frequency ranges.

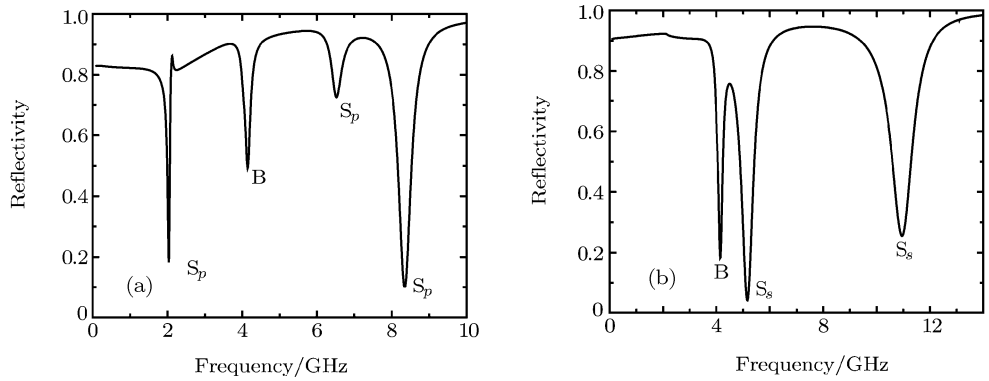


Fig. 11. The same as Fig. 3. Asymmetric slab is comprised of NMPM, LHM, and NDPM. Panel (a) shows the reflectivity for p polarization with $a = 0.5$ cm and panel (b) displays the reflectivity for s polarization with $a = 0.4$ cm. The other parameters used are $\varepsilon_0 = 3.0$, $\mu_0 = 1.0$, and $\theta_0 = 45°$.

Finally, we discuss the effect of the slab thickness on SPPs as shown in Fig. 12. From Fig. 10, which was calculated for a thickness of $h_0 d = 0.5$ it follows that when this slab thickness increases, in a low frequency range, the p-polarized branch (P1) is almost unchanged, but in a high frequency range, the separation between the p-polarized branches (P2) and (P3) decreases, but the separation between the s-polarized branches (S1) and (S2) increases as demonstrated in Fig. 12(a), which was calculated for a thickness of $h_0 d = 1.5$. In contrast, when this slab thickness decreases, the separation between the p-polarized branches (P2) and (P3) increases, but the separation between the s-polarized branches (S1) and (S2) decreases as demonstrated in Fig. 12(b),

which was calculated for a thickness of $h_0 d = 0.1$. These results are very interesting and quite different from those presented by Ruppin.[22]

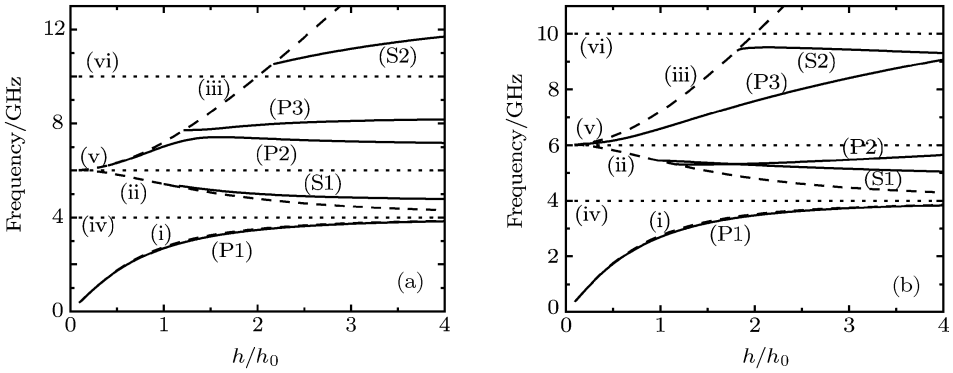


Fig. 12. The same as Fig. 10. Dispersion-relation curves for two different thicknesses of the NMPM–LHM–NDPM asymmetric slab, i.e. $h_0 d = 1.5$ (a) and 0.1 (b).

According to the above discussion, we find that different slabs have different SPPs. We also observe that the branches of p- or s-polarized SPPs occur in quite different frequency ranges because the jumps of the permittivity and the permeability from positive to negative are different across the two surfaces of the asymmetric slabs. In addition, for the above asymmetric slabs, surface polaritons exist only in the frequency stop band (in which both the permittivity and the permeability are not simultaneously negative or positive).

5. Conclusions

The p- and s-polarized SPPs of symmetric and asymmetric various slabs formed arbitrarily by four types of different materials: dielectrics, NDPMs, NMPMs, and LHMs, are investigated. Two symmetric slabs and three asymmetric slabs are examined in detail. The existence regions and the dispersion-relation curves of p- and s-polarized SPPs in the frequency regime are analysed, the possibility of exciting and observing SPPs by using the ATR technique are discussed, and the ATR spectra for both p- and s-polarization cases for these slabs are calculated. It is shown that the properties of SPPs for different slabs are quite different. The existence regions of SPPs, the numbers and the frequency positions of surface polariton branches, and the locations of ATR peaks are strongly dependent on the system structure, such as, the composite materials and the thickness of the slab, the parameters of metamaterials, etc. So the properties of SPPs can be controlled by choosing an appropriate system structure. All the results about SPPs may have some possible applications to the designs of novel lenses and filters based on metamaterials.

References

[1] Veselage V G 1968 *Sov. Phys. Usp.* **10** 509

[2] Pendry J B, Holden A J, Stewart W J and Youngs I 1996 *Phys. Rev. Lett.* **76** 4773

[3] Pendry J B, Holden A J, Robbins D J and Stewart W J 1998 *J. Phys.* **10** 4785

[4] Pendry J B, Holden A J, Robbins D J and Stewart W J 1999 *IEEE Trans. Microwave Theory Tech.* **47** 2075

[5] Smith D R, Padilla W J, Vier D C, Nemat-Nasser S C and Schultz S 2000 *Phys. Rev. Lett.* **84** 4184

[6] Shelby R A, Smith D R and Schultz S 2001 *Science* **292** 77

[7] Martel J, Marqués R, Baena J D, Medina F, Falcone F, Sorolla M and Martín F 2003 in *Progress in Electromagnetics Research Symposium* (PIERS) p. 194

[8] Shi H Y, Jiang Y Y, Sun X D, Guo R H and Zhao Y P 2005 *Chin. Phys.* **14** 1571

[9] Dong Z G, Zhu S N and Liu H 2006 *Chin. Phys.* **15** 1772

[10] Marqués R, Martel J, Mesa F and Median F 2002 *Phys. Rev. Lett.* **89** 183901

[11] Padilla W J, Smith D R and Basov D N 2006 *J. Opt. Soc. Am.* B **23** 404

[12] Rockstuhl C, Zentgraf T, Pshenay-Severin E, Petschulat J, Chipouline A, Kuhl J, Pertsch T, Giessen H and Lederer F 2007 *Opt. Express* **15** 8871

[13] Alù A and Salandrino A and Engheta N 2006 *Opt. Express* **14** 1557

[14] Hoffman A J, Alekseyev L, Howard S S, Franz K J, Wasserman D, Podolskiy V A, Narimanov E E, Sivco D L and Gmachl C 2007 *Nature Materials* **6** 946

[15] Barnes W L, Dereux A and Ebbesen T W 2003 *Nature* **424** 824

[16] Otto A 1968 *Z. Phys.* **216** 398

[17] Otto A 1969 *Z. Phys.* **219** 227

[18] Nkoma J S 1993 *Solid State Commun.* **87** 241

[19] Gaspar-Armenta J A and Villa F 2003 *J. Opt. Soc. Am.* B **20** 2349

[20] Darmanyan S A, Nevière M and Zayats A V 2004 *Phys. Rev.* B **70** 075103

[21] Ruppin R 2000 *Phys. Lett.* A **277** 61

[22] Ruppin R 2001 *J. Phys.* **13** 1811

[23] Shadrivov I V, Sukhorukov A A and Kivshar Y S 2004 *Phys. Rev.* E **69** 016617

[24] Darmanyan S A, Nevière M and Zakhidov A A 2003 *Opt. Commun.* **225** 233

[25] Zhang H X, Bao Y F, Lü Y H, Chen T M and Wang H X 2008 *Chin. Phys.* B **17** 1645

[26] Podolskiy V A, Sarychev A K and Shalaev V M 2003 *Opt. Express* **11** 735

[27] Pendry J B 2000 *Phys. Rev. Lett.* **85** 3966

[28] Cao D, Zhang H F and Tao F 2008 *Acta Opt. Sin.* **28** 1601 (in Chinese)

[29] Zhang H F, Wang Q, Shen N H, Li R, Chen J, Ding J P and Wang H T 2005 *J. Opt. Soc. Am.* B **22** 2686

[30] Tao F, Zhang H F, Yang X H and Cao D 2009 *J. Opt. Soc. Am.* B **26** 50

[31] Kretschmann E 1971 *Z. Phys.* **241** 313

[32] Kliewer K L and Fuche R 1966 *Phys. Rev.* **144** 495